Design of an Apparatus for Experimental Validation of the Plasma Kinetic Model for Electrostatic Discharge

by

Matthew David Webb

Undergraduate Honors Thesis

Presented to the Faculty of the Cockrell School of Engineering of

The University of Texas at Austin

in Partial Fulfillment

of the Requirements

for the Degree of

Bachelor of Science in Mechanical Engineering

The University of Texas at Austin

May 2018

ACKNOWLEDGEMENTS

I will first thank the Weapon Surety and Military Liaison Group (W-10) as a whole for welcoming me into their group at Los Alamos National Laboratory. In particular, I would like to thank Jonathan Mace, Douglas Tasker, Bud Reed, and Zachary Hardy for their collaboration throughout the entire project. Their help and guidance was instrumental during the design, assembly, and testing process. I would also like to thank Justine Davidson for her continued mentorship and Dan Borovina for overseeing the project.

I will next thank Dr. Charles (Chip) Durfee and John Rose at Colorado School of Mines for their assistance during the design process, especially for providing valuable information regarding design restrictions.

I would also like to thank Dr. Sheldon Landsberger for his encouragement and guidance during my education and for serving as the first reader for this thesis. He has been an integral part in advancing my educational and personal goals as well as a good friend. I would also like to thank Dr. Robert Hebner for agreeing to be the second reader for this thesis.

Finally and most importantly, I would like to thank my mother, father, and sister for their love and support always.

Design of an Apparatus for Experimental Validation of the Plasma Kinetic Model for Electrostatic Discharge

by

Matthew David Webb

The University of Texas at Austin, 2018

Electrostatic discharge (ESD) events are a serious safety concern when handling nuclear weapons. Current safety analysis operates under the assumption that sparks produced during threshold ESD events are overdriven and deliver all stored energy to a victim load. This assumption may result in safety procedures that are overly conservative unless a more accurate characterization can be made. Colorado School of Mines (CSM), in partnership with Los Alamos National Laboratory (LANL), has developed a plasma kinetic model for electrostatic discharge in COMSOL to model threshold ESD events from dielectric surfaces. The first experiment in a two experiment series aiming to validate this model involves quantifying the proportion of energy a target surface receives from a charged surface during a threshold ESD event. Experimental results will be compared to simulations run by CSM. This thesis covers the design of an experimental apparatus to be used in this first series of experiments.

TABLE OF CONTENTS

LIST OF FIGURES

LIST OF TABLES

Chapter 1: Introduction

1.1 Weapon Safety

The nuclear weapons complex faces many challenges during routine handling, maintenance, and storage processes. The safety of the operator and weapon must be of the utmost importance at all times. It is therefore necessary to follow stringent regulations and procedures when handling a weapon that take into account even the most unlikely of scenarios.

While it is impossible to account for every possible event or combination of events that a nuclear weapon may be exposed to, characterizing the response of a weapon to external forces has proven to be a significant factor in preventing accidents in the past (Schlosser, 2014). Some of the more common external forces include drops from various heights, exposure to fire or water, strikes from lightening or other electrical sources, and rapid changes in pressure, among others. Analyzing the conditions that a weapon may encounter can lead to design or procedural controls which are implemented to ensure the safety and reliability of the nuclear stockpile.

1.2 Electrostatic Discharge in the Weapons Complex

. Electrostatic discharge (ESD) events are an area of concern when handling nuclear weapons, especially during maintenance. Electrostatic discharge is a sudden flow of electricity between two bodies and is driven by a potential difference across charged and uncharged (target) surfaces (Greason, 1992). An ESD event imparts electrical energy to the target surface which then dissipates as heat.

Sparks can be categorized into two separate phenomena: overdriven and threshold. Overdriven sparks result from a sustained arc channel, the path electrons take to travel from the

charged surface to the target. A sustained arc channel is driven by a large and continuous potential difference across the surfaces during the discharge. As the arc channel increases the temperature of the medium, the resistance in the channel lowers and less energy is dissipated (Hyatt 1993). Because the arc channel is sustained, more energy is available to be delivered to the target as it is no longer being used to create the channel. An everyday example of this kind of spark would be that from a handheld taser. The power source in a taser provides a constant potential difference across its prongs thereby sustaining an arc channel and delivering a substantial amount of energy. In contrast, threshold ESD events occur the instant two surfaces have a great enough potential difference to overcome the dielectric strength of the medium between them without that energy being replenished by a power source. This spark is the kind most people associate with getting shocked by another person or object. As charge leaves the charged surface, the potential difference across the surfaces drops to the point that the arc channel closes and electrons stop flowing. As a result, it is expected that much of the energy during a threshold ESD event is used to create the arc channel rather than delivered to the target surface (Hyatt 1993).

Should an ESD event occur, it is possible the imparted energy could cause a detonator to fire, ignite high explosives (HE), or damage electronic components inside the weapon. Due to the risk that ESD events pose during routine operations, there are controls in place to reduce the likelihood of unintentional discharges. These controls may be overly conservative in that they expect the spark from an ESD event would behave similarly to an overdriven spark rather than a threshold event. It is currently assumed that all available stored energy is delivered from the charged surface to the target surface. This would mean that the charged surface must also be a

perfect conductor and all charge participates in the ESD event. This may be inaccurate for dielectric surfaces where charge can take a significant amount of time to disperse evenly.

1.3 The Plasma Kinetic Model for Electrostatic Discharge

The Department of Physics at Colorado School of Mines (CSM), in collaboration with W-10 at Los Alamos National Laboratory (LANL), has developed a model in Computational Multiphysics Solver (COMSOL) that aims to address the assumptions about the nature of threshold ESD events. Their model tackles the assumptions that all charge participates in the event and that all available energy is delivered to the victim by solving the full set of Maxwell's equations and incorporating a plasma kinetic model to describe an arc channel breakdown in air (Webb, Hardy 2017).

1.4 Scope

Los Alamos National Laboratory will conduct a series of two experiments to investigate the validity of the model produced by CSM. Each experiment will focus on one of the two aforementioned assumptions about threshold ESD events. The first experiment will quantify the energy delivered to the target surface and compare it to the available stored energy. The second experiment will target the amount of charge from a dielectric surface that participates in a threshold ESD event. The scope of this thesis covers the design of the apparatus to be used during the first experiment.

1.5 Thesis Objective

The objective of this thesis project was to design, assemble, and test an apparatus that can be used to quantify the amount of energy imparted to a target surface during a threshold ESD event. Given that the experimental series is still ongoing at LANL, only the design of the apparatus will be covered.

Chapter 2: Experimental Validation

2.1 Experimental Objective

The objective for the first experiment in the ESD series is to quantify the energy imparted to a target surface during a threshold ESD event and compare it to the available energy to obtain a proportion of transferred energy. The results will then be compared to those obtained using the plasma kinetic model developed by CSM. The model can be considered validated if its results agree with those from the experiments and are appropriately conservative.

2.2 Experimental Setup

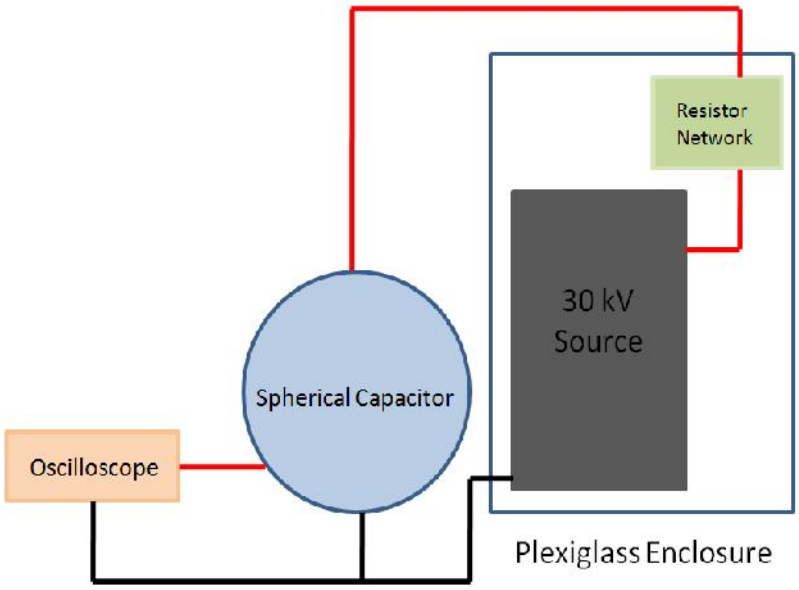

Figure 1: Experimental Setup Diagram

The experimental setup is based on a spherical capacitor system. A 30,000 Volt source passes current through a large resistance resistor network to slowly charge the inner sphere of the capacitor until it has a great enough potential difference between it and the grounded outer

sphere to discharge through the medium, air, between the spheres. The inner sphere will produce a discharge arc to a target surface embedded in the grounded outer sphere. At the moment of discharge, there will be a current in the target surface as it receives electrons from the charged inner sphere that can be measured with the oscilloscope. The current profile is then used to quantify the imparted energy received by the target surface. Given that the spherical capacitor will be a conductor, the geometry of the capacitor and dielectric strength of the medium can be used to calculate the stored energy at the time of breakdown. Once breakdown inside the spherical capacitor occurs, a large resistance resistor network ensures the capacitor will not reach breakdown voltage again before the arc channel has time to close, resulting in a threshold ESD event rather than one that is sustained and overdriven. The plexiglass and grounded outer sphere enclose all high voltage components, making the setup safe to operate.

2.3 CSM Model Results

The experimental setup and apparatus part files were supplied to Colorado School of Mines for modeling. CSM performed simulations for 2D axisymmetric models and produced expected current profiles and energy transfer at various breakdown voltages. Their model suggests a rise time between 1 and 3.5 nanoseconds with a peak current ranging from 250 to 1,000 Amperes. The simulated results are further summarized in Figure 2 and Table 1 on the next page.

Table 1: Fraction of Stored Energy Transferred to the Target Surface

Breakdown Voltage [kV]	Energy to Victim Load [%]
15	1.03
20	1.92
25	2.47
30	3.43

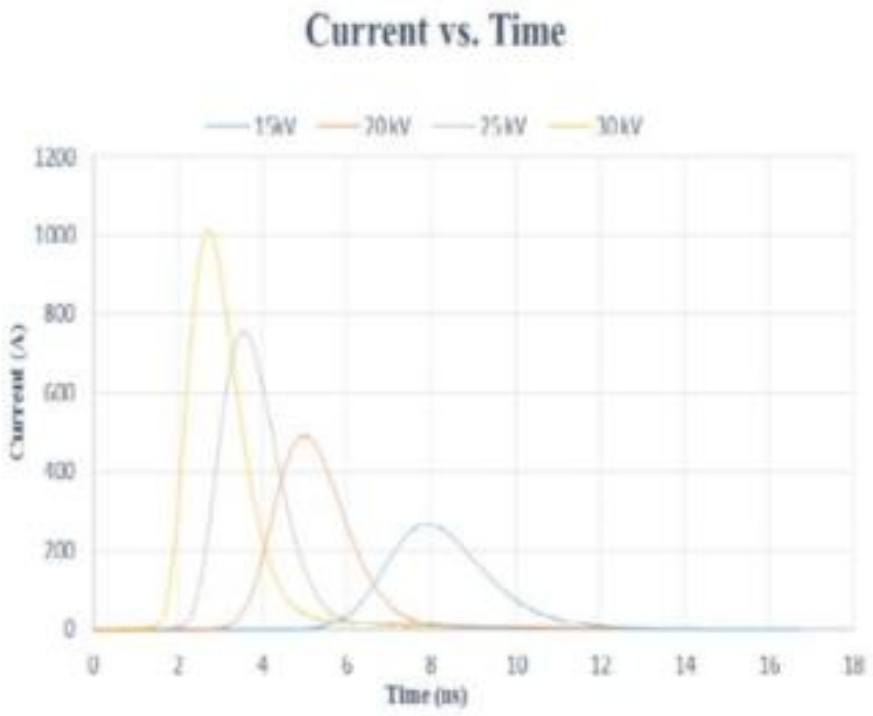

Figure 2: Current Profiles for Various Breakdown Voltages

Chapter 3: Apparatus Design

The major features of the experimental setup are outlined in Figure 1. This diagram and corresponding summary gives a holistic overview of each component's function. However, the method for achieving each function presented several challenges. Some of the major components, to include the 30,000 Volt power supply, resistor network, and oscilloscope, were ready made and are therefore outside the scope of this thesis. This chapter will discusses in depth the design of the experimental apparatus and its components, represented in the experimental setup diagram as the spherical capacitor.

3.1 Requirements

Both experimental series require a charged surface to discharge to a predefined target surface. The current through that target surface must pass through a known load and measured so that the energy deposition can be calculated.

Although there were no firm requirements set on size, weight, or component number, it was decided that the apparatus should be able to be moved and disassembled easily by one person in order to aid storage and transport. Furthermore, it was required that the apparatus be airtight in an effort to reduce foreign particles in the air gap of the capacitor.

In addition to the best-practices set of requirements for most design projects, there were a couple functional requirements inherent to the nature of the experiment. The most obvious requirement is that the apparatus must be able to charge to 30,000 Volts in an enclosed environment. An enclosed grounded system removes the danger of electric shock to the operators during normal procedure. While it is always advisable to try to remove exposure to

high voltage whenever possible, it could not be helped in this situation as a high potential difference is required to achieve breakdown in air.

Another clear requirement is that the location of the ESD event or breakdown must be guaranteed and must not be the outer grounded sphere. As previously stated, the grounded enclosure serves as a safety device against high voltage shocks. It is therefore unacceptable to have that surface become charged as it would pose a safety risk.

The most critical requirements that needed to be met were related to successful operation of the experiment- ability to charge and location of discharge- and were the focus of the majority of the design choices as a result.

3.2 Summary of Final Assembly

Given that the apparatus consists of several unique components, it is best to overview the final design as a whole before reviewing the design choices for the individual components in depth. A center-plane cross section of the apparatus, Figure 3, can be found on the following page.

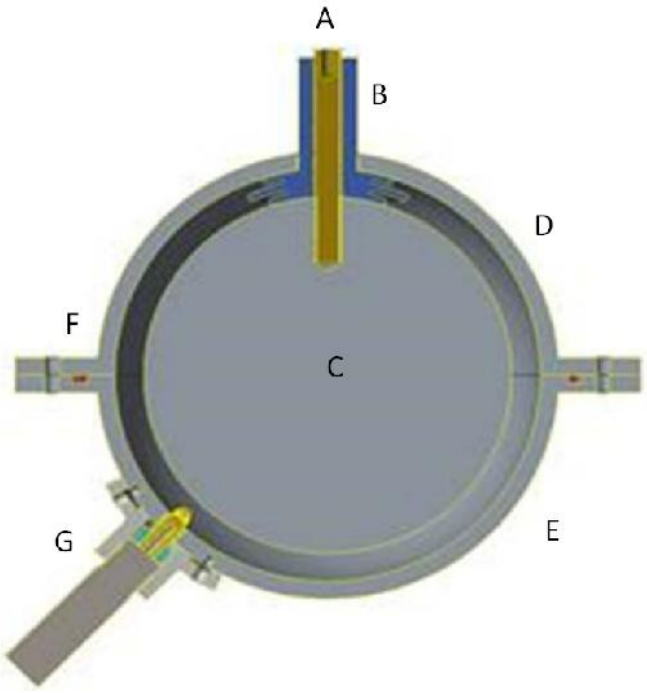

Figure 3: Center-plane Cross Section

The final design for the apparatus consists of a solid aluminum inner sphere (C) 5 inches in diameter enclosed by two aluminum hemispheres (D, E) joined about the inner sphere's equator and leaving a 0.394 inch (1.00 cm) gap all around. The enclosure is sealed using an o-ring (F) placed in a depth controlled groove in the bottom hemisphere and compressed by four screws that affix the top hemisphere to the bottom hemisphere. The inner sphere is held in place using the spherical mating surfaces of the top insulating piece (B) and charged with a brass rod (A) passing through the center of the insulator and into a threaded hole in the inner sphere. An insulating nut (not shown) screws down over the outer diameter of the insulator, compressing the top insulator to the outer sphere while a standard machined nut (not shown) screws down over the brass charging rod, compressing the inner sphere to the bottom mating surface of the insulator. This system guarantees the concentricity of the inner sphere relative to the outer sphere within a tight tolerance.

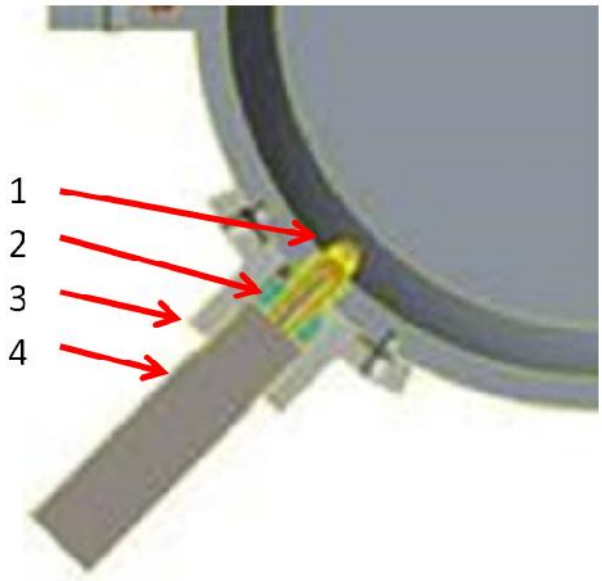

Figure 4: Target Rod Assembly Center Plane Cross Section

The target rod assembly (G), shown in Figure 4, is attached to the outer sphere in a specific order. The aluminum target housing (3) is fixed to the outer sphere using standard screws. The target rod (1) is then pressed into the target insulator (2) before being screwed onto the end of the current viewing resistor (4). The current viewing resistor is then screwed into the target housing, using the housing to align the target insulator into a threaded hole in the bottom hemisphere and placing the target rod into the gap between the spheres. The target rod protrudes into the electric field enough that it is energetically favorable for the inner sphere to discharge to that surface. The current then passes through the resistor and is measured using the oscilloscope. While a procedure of assembly is generally undesirable, this process is very helpful for placing the target rod in the correct location. The alternative method involves screwing the target insulator into the bottom hemisphere by hand, which makes it very difficult to guarantee positional accuracy due to the outer hemisphere's curved outer surface.

3.3 Inner and Outer Spheres

Given that the capacitance of the capacitor needs to be known in order to calculate the stored energy, the possible geometries the capacitor could realistically be was limited to three options: parallel plates, concentric cylinders, and concentric spheres. Parallel plates could then be excluded due to the requirement that the system be enclosed for safety reasons. While the formula for the capacitance of concentric cylinders is readily available, the charge distribution on a cylinder would not be uniform as charge tends to accumulate at edges. In order to keep a uniform charge density across the entire surface and maintain an enclosed system with an easy to calculate capacitance, as spherical geometry was determined to be ideal.

This apparatus will be primarily used for the first of a series of two experiments. The first series aims to quantify the amount of energy deposited on a target surface from a charged surface during a threshold ESD event. Because the experiment is focusing on energy deposition rather than proportion of participating charge as in the next series, a conductive material can be used for the capacitor. Aluminum and stainless steel were considered for the capacitor material due to their availability, cost, and conductive properties.

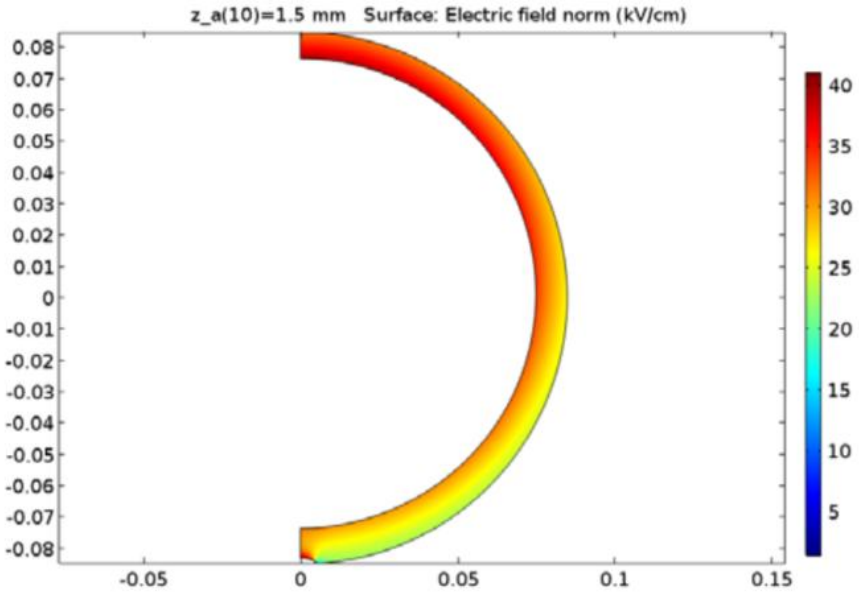

Figure 5: CSM 1.5mm Z-Offset Electromagnetic Field Calculations

It was initially thought that spun metal hollow spheres would be sufficient for the inner and outer spheres as it is not necessary to have a solid inner sphere since charge accumulates at the outer surface of a charged body. However, concentricity offset calculations of the kind shown in Figure 5 performed by CSM show that offsets in one axis on the order of millimeters can drastically alter the electric field in the capacitor. Given enough offset from perfectly concentric, it would not be guaranteed that the ESD event would breakdown to the desired target surface. After running several simulations, CSM recommended a concentricity offset of no more than 0.020 inches (0.5 millimeters). This became a driving factor for several design decisions moving forward. It was clear that the spun spheres would not have the dimensional tolerance necessary, and after speaking with LANL machinists, it was determined that spun spheres could not be post machined to tolerance due to their thin walls. The option with the tightest tolerance was to have a solid sphere machined out of aluminum with an outer diameter tolerance of 0.001 inches and two outer hemispheres machined from aluminum with an inner diameter tolerance of

0.001 inches as well. This resulted in a base tolerance stack of 0.002 inches, which was significantly less than that of spun spheres. In addition to the tight machining tolerance, the outer surface of the inner sphere and the inner surface out the outer hemispheres were polished to a mirror finish. This was done to further ensure charge would be more evenly distributed over the outer surface of the inner sphere and that the target rod would be the greatest protrusion into the electromagnetic field between the two.

3.4 Insulators

The purpose of an insulator is to electrically isolate two surfaces or mediums. The dielectric strength of an insulator describes the potential difference it can withstand without breaking down per unit length of the insulator medium. This experiment presented a significant challenge with isolating components since it involved charging surfaces to up to 30,000 Volts. At such a high voltage, bulk breakdown, discharge through the insulator medium, and surface breakdown, discharge over the exterior of the insulator, are serious concerns. Because the inner sphere must be charged via an external brass charging rod, the charging rod must not touch the outer sphere, and the most likely location for breakdown is where the charging rod passes near the opening of the outer sphere. It is therefore necessary to insulate the charging rod from discharging to the outer sphere. A model performed my CSM of the electric field near this area is shown on the following page in Figure 6.

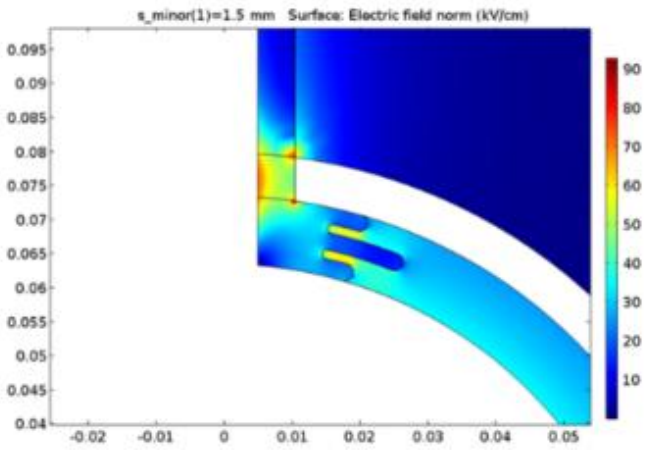

Figure 6: CSM Electromagnetic Field Calculations for Finned Insulator

The two bright red points in the image show where the electromagnetic field is strongest and is therefore the most likely location for breakdown. Although breakdown was not expected, the insulator that did fail, to be discussed further on in this section, did so at the bottom most red point where the insulator meets the inner edge of the outer sphere.

Figure 7: Top Insulator and Cross Section 3D Print

An insulator was initially designed with the cross section shown in Figure 7. In an effort to prevent surface breakdown along the insulator's surface from where it contacts the inner sphere to where it contacts the outer sphere, an extended fin was added to increase the required

surface path. Increasing the distance charge must travel reduces the likelihood that surface breakdown will occur at a given voltage. However, the geometry of the cutouts that shape the extended fin is not easily machined using traditional methods.

Additive manufacturing can remove many geometric restrictions typical of traditional machining. Given the unusual shape of the insulator, it was decided to 3D print the insulator out of ABS plastic using a solid fill. ABS plastic has a dielectric strength of 450,000 Volts/inch, so the 3D printed insulator should have withstood 86,000 Volts before bulk breakdown (Overview, n.d.). However, initial testing resulted in the insulator failing near 9,000 Volts through the bulk of the material (Webb, Hardy, 2017). It is strongly suspected the 3D printing process negatively affected the electrical insulating propertied of the ABS plastic. With this in mind, the insulator was altered so that it could be machined out of Delrin or Teflon using traditional methods. The machined insulator and its cross section are shown in Figure 8 below.

Figure 8: Top Insulator and Cross Section Machined

Two separate insulators were designed, but both were dual-purpose. CSM's concentricity analysis revealed that it was critical the centers of the inner and outer spheres be within 0.020 inches (0.5 millimeters) in any given direction or risk discharge to unintended locations. As a result, the insulating components needed to serve as alignment tools as well.

The top insulator, seen in Figure 7 and Figure 8 sets the gap between the outer surface of the inner sphere and the inner surface of the outer sphere using its two spherical surfaces. The radial distance between the two surfaces is exactly .394in or (1 cm) and has a tolerance of 0.005 inches if machined additively or as small as 0.001 inches if machined using a lathe.

Similar to the first top insulator, the target insulator shown in Figure 4, was also 3D printed ABS plastic with a solid fill. However, this insulator is not expected to experience the same bulk breakdown issue. Because the target insulator in insulating the target rod from the outer sphere rather than the charging rod, it is expected to see only a small percentage of the potential difference that the top insulator faced. This is, after all, the basis for the first experimental series.

4.5 Target Assembly

The target rod assembly, seen in Figure 4 consists of four components and is oriented at 45 degrees from the axis of the charging rod. In order to obtain more meaningful results, the location of the ESD event must be consistent and the path length to the diagnostics must be minimized. The target rod, a brass, elliptical tipped rod, perturbs the electromagnetic field between the inner and outer spheres just enough to ensure it is always energetically favorable for breakdown to occur at that point. Simulations run by CSM indicate that an elliptical tipped target rod would be the most favorable tip geometry for channeling the breakdown. Several

target rods were machined from 0.25in diameter brass stock with semi-elliptical tips having minor-axis ranging from 1mm to 5mm. A simulation of the electromagnetic field near a semi-elliptical tipped target rod is shown in Figure 4.5 below.

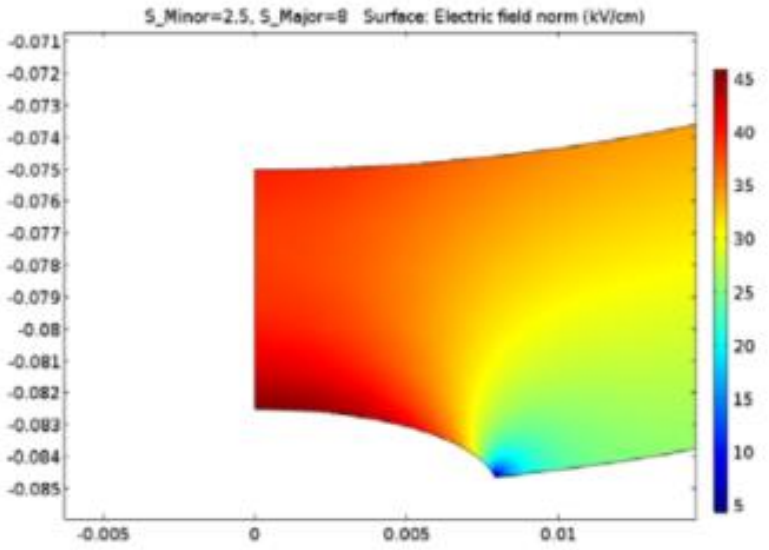

Figure 9: CSM Electromagnetic Field Calculation for a 2.5mm Semi-Minor Axis Target Rod

The target insulator holds the target rod in place in the outer sphere. As previously discussed, it is not expected that the target rod will see a high enough potential difference to compromise the 3D printed insulator. In this case, it is satisfactory that the target rod simply not touch the grounded outer sphere.

For the current viewing resistor (CVR) to measure the current through the target rod, it must be in contact with the electrically isolated target rod and have a ground reference. The connection to the ground reference is achieved using the target assembly housing. The aluminum housing holds the CVR in place in the outer sphere and serves as a conductive connection to the grounded outer sphere. This part needed to be specifically designed to be machined on a lathe due to its spherical mating surface with the outside of the outer sphere.

Although this was a challenge, it allows the part to serve as an alignment tool when placing the target rod into the gap between the spheres. Because the target rod enters the spherical enclosure at an angle, it is very easy to misalign the target when placing it by hand.

Chapter 4: Conclusions and Future Work

This apparatus is currently being used at Los Alamos National Lab (LANL) to perform the first of a two part series of experiments to better characterize electrostatic discharge events. Should preliminary experimental results agree with the 2D simplified simulations performed by CSM, full 3D simulations will be produced in an effort to validate the plasma kinetic model.

Future work involves tackling the assumption that all charge from a dielectric surface participates in an ESD event. It is likely a modified version of the apparatus discussed in this thesis will be used for this second series of experiments.

References

Greason, W. (1992). Electrostatic discharge: A charge driven phenomenon. Journal of Electrostatics, 28(3), 199-218. doi:10.1016/0304-3886(92)90073-3

Hyatt, H. M. (1993). The resistive phase of an air discharge and the formation of fast risetime ESD pulses. Journal of Electrostatics, 31(2-3), 339-356. doi:10.1016/0304-3886(93)90017-2

Overview of materials for Acrylonitrile Butadiene Styrene (ABS), Extruded. (n.d.). Retrieved March 19, 2018, from http://www.matweb.com/search/DataSheet.aspx?MatGUID=3a8afcddac864d4b8f58d40570d2e5aa

Schlosser, E. (2014). Command and control: Nuclear weapons, the Damascus Accident, and the illusion of safety. New York: Penguin Books.

Webb, M. D., & Hardy, Z. K. (2017). Experimental Validation of the Plasma Kinetic Model (Working paper). Los Alamos, NM: Los Alamos National Laboratory.